Transport in Josephson junctions with a graphene interlayer

Matti Tomi,[1] Mikhail R. Samatov,[2] Andrey S. Vasenko,[3,4]
Antti Laitinen,[1] Pertti Hakonen,[1,5] and Dmitry S. Golubev[1]

[1] *QTF Centre of Excellence, Department of Applied Physics, Aalto University, P.O. Box 15100, FI-00076 Aalto, Finland*
[2] *National Research University Higher School of Economics, 101000 Moscow, Russia*
[3] *HSE University, 101000 Moscow, Russia*
[4] *I.E. Tamm Department of Theoretical Physics, P.N. Lebedev Physical Institute, Russian Academy of Sciences, 119991 Moscow, Russia*
[5] *Low Temperature Laboratory, Department of Applied Physics, Aalto University, P.O. Box 15100, FI-00076 Aalto, Finland*

We study, both theoretically and experimentally, the features on the current-voltage characteristic of a highly transparent Josephson junction caused by transition of the superconducting leads to the normal state. These features appear due to the suppression of the Andreev excess current. We show that by tracing the dependence of the voltages, at which the transition occurs, on the bath temperature one can obtain valuable information about the cooling mechanisms in the junction. We verify theory predictions by fabricating two highly transparent superconductor-graphene-superconductor (SGS) Josephson junctions with suspended and non-suspended graphene as an interlayer between Al leads. Applying the above mentioned technique we show that the cooling power of the suspended junction depends on the bath temperature as $\propto T_{\rm bath}^3$ close to the superconducting critical temperature.

I. INTRODUCTION

Highly transparent Josephson junctions possess unique properties distinguishing them from the usual low-transparency junctions, in which two superconducting leads are separated by a tunnel barrier. For example, transparent junctions have a non-sinusoidal current-phase relation [1, 2] and host Andreev levels, which can be probed by microwave spectroscopy [3] and can be potentially used for quantum information processing [4]. These junctions also exhibit a characteristic pattern of multiple Andreev reflection peaks in the differential conductance at sub-gap bias voltages $eV < 2\Delta$, where Δ is the superconducting gap [5–8]. Two superconducting leads of a transparent Josephson junction are usually connected by a short section made of a non-superconducting material, which forms good electric contacts to them. A variety of materials have been used for this purpose: carbon nanotubes [9–11], graphene [12, 13], InAs nanowires [3, 14, 15], 2d [16] and 3d [17, 18] topological insulators.

Here we consider yet another characteristic feature of highly transparent Josephson junctions – the excess current. More specifically, we investigate, both theoretically and experimentally, the suppression of the excess current by Joule heating. It is known that the I-V curve of a transparent junction at high bias voltage approaches the asymptotic form $I = V/R + I_{\rm exc}$, where R is the junction resistance in the normal state and $I_{\rm exc}$ is the excess current. This current is proportional to the value of the gap Δ in the leads and originates from Andreev reflection [19]. Joule heating of the superconducting leads suppresses the gap Δ. At some bias point the temperature of the leads reaches the critical temperature of the superconducting phase transition T_C, and both the gap and the excess current vanish. This bias point is marked by a dip in the differential conductance of the junction. Such dips are often observed in experiments, but, to the best of our knowledge, they have not been yet systematically studied. We show that the position of the dip in the differential conductance provides important information about cooling mechanisms in the junction, and derive a simple analytical expression for the differential conductance in the vicinity of the dip. Next, we test the theory predictions experimentally by studying highly transparent superconductor - graphene - superconductor (SGS) Josephson junctions with aluminum leads. Graphene is known to be a very promising material for bolometry [20–27]. Recently, bolometers based on SGS junctions similar to ours and having the noise equivalent power at the level $10^{-20} - 10^{-18}$ W/$\sqrt{\rm Hz}$ in the microwave frequency range have been demonstrated [28, 29]. We argue that the technique based on the suppression of the excess current by Joule heating may provide an additional simple tool for calibration of such bolometers.

The paper is organized as follows: in Sec. II we present the theoretical model, in Sec. III we discuss the experiment and in Sec. IV we summarize our results.

II. MODEL

In this section we present the theoretical model. We assume that the bias voltage V applied to the junction is positive and sufficiently large, $eV > 2\Delta$. In this limit the I-V curve of a transparent Josephson junction can be well approximated as

$$I(V) = \frac{V}{R} + \alpha \frac{\Delta_L(T_L) + \Delta_R(T_R)}{2eR}. \qquad (1)$$

Here the second term in the right hand side is the excess current and $\Delta_L(T_L)$ and $\Delta_R(T_R)$ are the superconducting gaps in the left and the right leads. They depend on the temperatures of the leads at the contacts with the central section, T_L and T_R. For a short Josephson junction with the distance between the leads, $L_{\rm jct}$, much shorter than the superconducting coherence length ξ, i.e. for $L_{\rm jct} \ll \xi$, the pre-factor α is expressed as [30]

$$\alpha = \frac{\sum_j \frac{\tau_j^2}{1-\tau_j}\left(1 - \frac{\tau_j^2}{2\sqrt{1-\tau_j}(2-\tau_j)} \ln\frac{1+\sqrt{1-\tau_j}}{1-\sqrt{1-\tau_j}}\right)}{\sum_j \tau_j}. \quad (2)$$

Here τ_j is the transmission probability of j-th conducting channel and the sums run over all channels. The parameter α varies between 0 and 8/3 and approaches its maximum value in a highly transparent junction with channel transmissions close to 1. In a tunnel junction with very small transmissions $\tau_j \ll 1$ one finds $\alpha \ll 1$ and the excess current in Eq. (1) vanishes. Two other important cases - a normal metal diffusive interlayer and a clean short and wide strip of graphene - are characterized by Dorokhov's distribution of transmission probabilities [33, 34], which results in $\alpha = \pi^2/4 - 1 \approx 1.4674$. Finally, in a junction having a long diffusive section with $L_{\rm jct} > \xi$ the pre-factor α decreases with the length as [35]

$$\alpha = 2.47\,\xi/L_{\rm jct}. \quad (3)$$

We first consider a simple case of the two identical superconducting leads, which are symmetrically coupled to the central normal section. Accordingly, we put $T_L = T_R = T_0$ and $\Delta_L(T_L) = \Delta_R(T_R) = \Delta(T_0)$. In order to find the dependence of the temperature T_0 on the bias voltage V we need to solve the heat balance equation

$$P(T_0, T_{\rm bath}) = IV, \quad (4)$$

where we have introduced the bath temperature $T_{\rm bath}$ and the cooling power of the sample $P(T_0, T_{\rm bath})$, which is, in general, unknown. The Joule heating power is partially carried away to the superconducting leads, while the rest of it goes to the substrate phonons and possibly to some other cooling channels, see Fig. 1a. At certain bias voltage V_C the contact temperature becomes equal to the critical temperature of the superconductor, $T_0 = T_C$. At this point the differential conductance has a dip. Tracing the position of this dip at different bath temperatures, one can restore the cooling power $P(T_C, T_{\rm bath}) = I(V_C)V_C$ as a function of $T_{\rm bath}$.

We now find the shape of the dip close to the critical voltage value V_C. In the vicinity of this bias point one can linearize Eq. (4) writing it in the form

$$G_C^{\rm th}(T_0 - T_C) = IV - I(V_C)V_C. \quad (5)$$

Here $G_C^{\rm th} = \partial P(T_0, T_{\rm bath})/\partial T_0|_{T_0=T_C}$ is the effective thermal conductance of the structure at critical temperature. According to the theory by Bardeen, Cooper and Schrieffer [36] (BCS), in the vicinity of the critical temperature

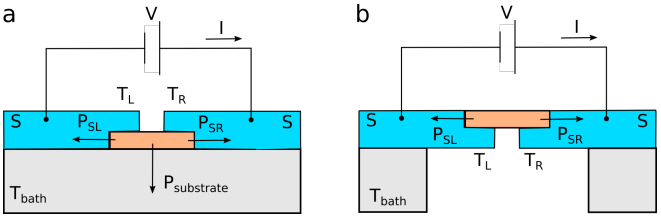

FIG. 1. (a) High transparency Josephson junction with normal-conductor section connecting the two identical superconducting leads, fully residing in contact with the substrate. Part of the Joule heat goes to the substrate ($P_{\rm substrate}$) and the rest of it – to the left (P_{SL}) and to the right (P_{SR}) superconducting leads. T_L and T_R are the temperatures of the superconducting leads at the contacts with the central section. (b) Josephson junction with a suspended interlayer, in which the Joule heat escapes only through the superconducting leads.

the superconducting gap behaves as

$$\Delta(T_0) = k_B T_C \sqrt{\frac{8\pi^2}{7\zeta(3)} \frac{T_C - T_0}{T_C}}, \quad (6)$$

where $\zeta(x)$ denotes Riemann's zeta function. Combining this expression with the expression for the I-V curve (1), we transform Eq. (5) to the form

$$G_C^{\rm th}(T_0 - T_C) = \frac{V^2 - V_C^2}{R} + \frac{k_B T_C V}{eR}\sqrt{\frac{8\pi^2\alpha^2}{7\zeta(3)} \frac{T_C - T_0}{T_C}},$$

Solving this equation for T_0, substituting the result in the expression for the current (1) and taking the derivative of it, we obtain a simple analytical expression for the differential conductance

$$\frac{dI}{dV} = \frac{1}{R} - \frac{4\theta(V_C - V)}{bR}\left(\frac{(b-4)V}{\sqrt{bV_C^2 - (b-4)V^2}} + 2\right) \quad (7)$$

Here $\theta(x)$ is the Heaviside step function and we have introduced the dimensionless parameter

$$b = \frac{14\zeta(3)}{\pi^2\alpha^2}\frac{e^2 R G_C^{\rm th}}{k_B^2 T_C}. \quad (8)$$

The approximation (7) is formally valid if $b \gg 1$ and $|V_C - V| \lesssim \alpha k_B T_C/e$. However, Eq. (7) can also be used outside this voltage interval because the non-linear correction to dI/dV almost vanishes there. Eq. (7) predicts strong dip in the differential conductance with the negative minimum value $-1/R$ achieved at $V = V_C$. In the experiment, the dip is smeared by the inhomogeneity of the hot spot in the contact area between the leads and the central section, by the inverse proximity effect suppressing the gap close to the contact, etc.

In reality the two superconducting leads of the junction are never fully identical. They may have different critical temperatures, different geometry, and different couplings to the central section. As a result, a single dip in dI/dV

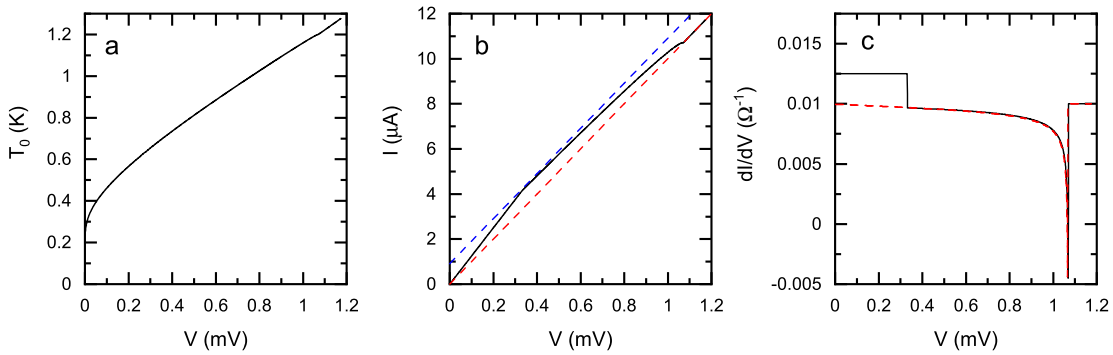

FIG. 2. Black solid lines show: (a) the dependence of the contact temperature T_0 on the bias voltage, (b) I-V curve of the junction with the supeconducting branch at $V = 0$ not shown, and (c) the differential conductance obtianed by solving Eq. (12) numerically. In panel (b) red dashed line indicates Ohm's law $I = V/R$, and blue line – Ohm's law with added excess current, $I = V/R + \alpha\Delta(0)/eR$. In panel (c) red dashed line represents the approximate expression (7). The following parameters have been chosen for this simulation: $R = 100\ \Omega$, $R_{L_S} = 2\ \Omega$, $T_C = 1.2$ K, $\Delta(0) = 182\ \mu$eV, $\alpha = 0.5$, $T_{\rm bath} = 10$ mK.

splits into two dips occurring at different bias voltages V_{CL} and V_{CR}, at which the left and the right leads switch to the normal state. In this case Eq. (4) cannot be solved analytically. However, in the limit $b \gg 1$ one can rather accurately approximate the solution by the sum of two independent dips,

$$\frac{dI}{dV} = \frac{1}{R} - \frac{2\theta(V_{CL}-V)}{bR}\left(\frac{(b-1)V}{\sqrt{bV_{CL}^2-(b-1)V^2}}+1\right) - \frac{2\theta(V_{CR}-V)}{bR}\left(\frac{(b-1)V}{\sqrt{bV_{CR}^2-(b-1)V^2}}+1\right). \quad (9)$$

For a symmetric case $V_{CL} = V_{CR}$ and for $b \gg 1$ Eq. (9) coincides with the more accurate Eq. (7) everywhere except a narrow interval close to the minimum of the dip. Eq. (9) is valid if the two dips are sufficiently close and one can use the same parameter b (8) for both of them.

A. Suspended symmetric junction

In this subsection we consider a suspended junction in a symmetric configuration, in which the only cooling mechanism is the removal of heat through the superconducting leads, see Fig. 1b. This model can be easily solved numerically, and it allows us to test the analytical approximation (7). By symmetry, the power $IV/2$ is dissipated in each lead. We assume that the right lead has the shape of a one-dimensional wire with the cross-sectional area S. Then, the temperature profile in the right lead is determined by the heat diffusion equation

$$S\kappa_S(T)\frac{dT}{dx} = -\frac{IV}{2}, \quad (10)$$

where the themal conductivity of the leads is [37],

$$\kappa_S(T) = \frac{4k_B^2\sigma}{e^2}T\int_{\frac{\Delta(T)}{2k_BT}}^{\infty}\frac{x^2}{\cosh^2 x}dx. \quad (11)$$

Here we have introduced the conductivity of the superconducting material in the normal state σ. We assume that the contact with the interlayer is located at $x = 0$ so that $T(0) = T_0$, and at $x = L$ the superconducting wire contacts the bulk lead with the bath temperature, $T(L) = T_{\rm bath}$. Integrating Eq. (10) from 0 to L, we obtain the equation for the contact temperature T_0,

$$P_S(T_0, T_{\rm bath}) = I(V)V, \quad (12)$$

where

$$P_S = \frac{8k_B^2}{e^2R_{\rm leads}}\int_{T_{\rm bath}}^{T_0}dT\,T\int_{\frac{\Delta(T)}{2k_BT}}^{\infty}dx\frac{x^2}{\cosh^2 x} \quad (13)$$

is the power carried away by quasiparticles through both superconducting leads. In Eq. (12) we introduced the total resistance of the two leads in the normal state $R_{\rm leads} = 2L/\sigma S$. In this model, the heat conductance at critical temperature is determined by Wiedemann–Franz law, $G_C^{\rm th} = 2\pi^2k_B^2T_C/3e^2R_{\rm leads}$, and the dimensionless parameter (8) acquires the form

$$b = \frac{28\zeta(3)}{3\alpha^2}\frac{R}{R_{\rm leads}}. \quad (14)$$

Next, from Eq. (12) we find the value of the critical voltage V_C at low bath temperatures $T_{\rm bath} \ll T_C$,

$$V_C \approx \sqrt{RP_S(T_C,0)} = 0.829\sqrt{\frac{R}{R_{\rm leads}}}\frac{\Delta(0)}{e}, \quad (15)$$

where we have numerically evaluated the cooling power $P_S(T_C, 0)$ assuming the BCS dependence $\Delta(T)$.

In Fig. 2 we present numerically exact results obtained from Eq. (12). We have chosen $\alpha = 0.5$ and approximated the I-V curve as follows: $I(V) = (1+\alpha/2)V/R$ for $eV < 2\Delta$, and $I(V) = (V + \alpha\Delta/e)/R$ for $eV > 2\Delta$. We ignored multiple Andreev reflection features at subgap voltages because we focus at the voltages above the gap, i.e. at $eV > 2\Delta$. Voltage dependence of the contact temperature $T_0(V)$ and of the current $I(V)$ are shown in

	type	L	W	leads	d (nm)	$W_{\rm lead}$	N	T_C (K)
NS	ML	0.30	6.0	Ti/Al/Ti	10/50/10	0.6	2	0.58
S	BL	0.50	1.0	Ti/Al	10/70	1.2	4	0.77

TABLE I. Parameters of the two studied samples: NS - non-suspended, S - suspended; the types ML and BL refer to monolayer and bilayer graphene, respectively. L and W denote the sample length and width in micrometers, respectively. Column d indicates the thickness of the metal layers evaporated for the contacts, while $W_{\rm lead}$ denotes the lead width in μm and N is the effective number of leads for hat transport. Critical temperature T_C represents an average value of the superconducting transition temperatures observed on different leads.

Figs. 2a and 2b respectively. In Fig. 2c we compare the exact differential conductance with the approximate expression (7) and observe perfect agreement between them for all voltages $eV > 2\Delta$.

III. EXPERIMENT

Our back-gated devices were fabricated using exfoliated graphene on a SiO_2/Si wafer. The substrate was highly boron-doped Si (p^{++}/B, $\rho < 10$ mΩcm) which remains conducting down to mK temperatures. A layer of dry oxide with a thickness of $250 - 270$ nm was grown thermally on the substrate at a temperature of 1000°C. Before depositing graphene, alignment markers were patterned on the chips using optical lithography and evaporation of Ti and Au.

For suspended samples, we made graphene exfoliation on LOR resist [38]. After making the electrical contacts using electron beam lithography, the area to be suspended was irradiated using a high dose of electrons, developed in ethyl lactate, and washed in hexane. The electrical leads were made of aluminum/titanium sandwich structures. Titanium was evaporated at ultra high vacuum conditions which resulted in high transparency contacts to graphene. The presence of Ti lowered the superconducting transition temperature of the leads: in our second sample structure with a trilayer sandwich structure 10/50/10 nm of Ti/Al/Ti, the critical temperature was suppressed to half of the bulk value. The normal state resistance of the Al leads is $< 1\,\Omega/\mu$m, which means that the Joule heating by the measurement current will mostly take place in the SGS junction. For details of the structure and dimensions of the two samples see Table I.

The suspended sample (S in Table I) with four measurement leads is illustrated in Fig. 3. The width of measurement leads is 1.2 μm, i.e. the contact areas are more than two times larger than the size of the actual suspended part of the graphene. The bright looking sections of the horizontal leads in Fig. 3 are also suspended. Thus, the Joule heating generated in graphene has to propagate along suspended metallic leads over a distance of at least two microns before any cooling by the substrate through the LOR resist may take place. The arrows in the figure illustrate the flow of electrical current as well as the main directions of Joule heat escape from the sample. The critical temperature was slightly different for the four leads and the obtained T_C values varied between $T_C = 760 - 780$ mK (BCS gap $\Delta = 115 \ldots 118\,\mu$eV).

Measurements were carried out using two dilution refrigerators: a BlueFors prototype cryostat BF-SD125 and a commercial BlueFors BF-LD250. Most of the measurements were performed on the BF-LD250 cryostat with the lowest achievable base temperature of approx. 10 mK. Temperatures were measured with a RuO_2 resistor that had been calibrated against a Coulomb blockade thermometer [39]. An electrically shielded room with filtered power lines was employed to prevent electromagnetic interference and low-frequency electrical noise from affecting the weak signals before amplification. To limit the amount of thermal noise entering from room temperature to the sample, all dc lines were equipped with three-stage RC low-pass filters at the base temperature of the cryostat, with a cut-off frequency of $f_{co} \simeq 1$ kHz.

The electrical characteristics were obtained using regular low-noise measurement methods and lock-in techniques. We employed current bias through $1-100$ MΩ resistor, selected on the basis of the required current range (dependent on gate voltage V_g). The voltage across the sample was measured using an LI-75 low-noise preamplifier powered from lead batteries. Differential resistance at small audio frequency (around 70 Hz) was measured simultaneously with the DC characteristics using a Stan-

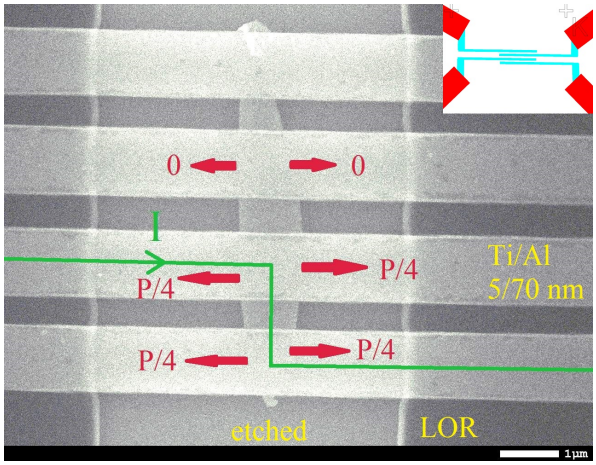

FIG. 3. Samples structure with the suspended (etched) part visible in the center between the vertical borders of the LOR resist seen as the darker background color. The Al/Ti measurement leads are seen as horizontal lighter grey stripes, the connection of which to the measurement system is displayed in the upper right corner. The green arrow depicts the electrical current flow in our experiments, while the red arrows illustrate the heat flows to the metallic leads as assumed in our analysis.

ford SR830 lock-in amplifier.

In Fig. 4 we show the IV curve of the non-suspended SGS junction. This junction has rather large excess current, which exceeds the Josephson critical current. For this reason, the suppression of the excess current at high bias voltage is clearly visible. The experimental I-V curve resembles the theoretical one plotted in Fig. 2b, although in the experiment only one of the leads becomes normal in presented range of bias voltages.

The superconducting-to-normal transition due to Joule heating in a suspended bilayer SGS sample is depicted in Fig. 5a for a temperature range of $10 \ldots 800\,\mathrm{mK}$ ($T_C \simeq 770\,\mathrm{mK}$). Each resistance peak is clearly split into two parts, presumably because of junction asymmetry. There is also a small asymmetry between positive and negative bias voltages, giving rise to a total of four peaks.

Heat flow in mesoscopic devices can typically be characterized by a power law of the form

$$P = \Sigma(T_{L,R}^{\gamma} - T_{\mathrm{bath}}^{\gamma}) \tag{16}$$

where Σ is a constant and γ is a characteristic exponent which depends on the dissipation mechanism. The transition to the normal state occurs at the critical temperature $T_{L,R} = T_C$ and the corresponding critical powers can be expressed as

$$P_C = \frac{P_{C,0}}{T_C^{\gamma}}(T_C^{\gamma} - T_{\mathrm{bath}}^{\gamma}), \tag{17}$$

where $P_{C,0}$ is the critical power for $T_{\mathrm{bath}} = 0$. The observed peak positions from Fig. 5a are plotted in Fig. 5b, along with fits using Eq. (17) and the exponent γ as a fit parameter. We obtain $\gamma \approx 3.1$ for all four peaks.

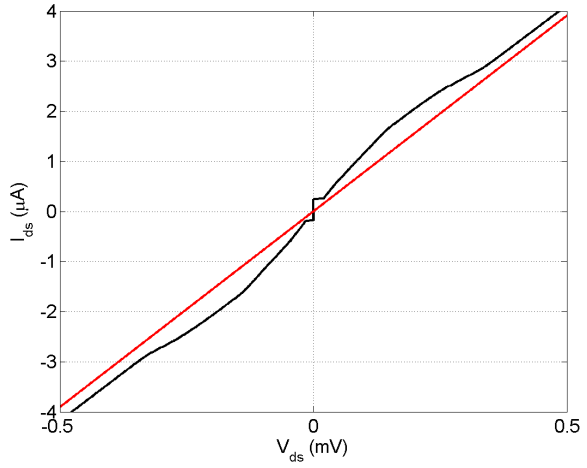

FIG. 4. Measured IV curve of sample NS at gate voltage $V_g = 30\,\mathrm{V}$ ($n \simeq 6 \times 10^{11}\,\mathrm{cm}^{-2}$) with the normal state resistance $R = 128\,\Omega$ (indicated by the red line). Parameters of the superconducting state: excess current just above the double gap voltage $I_{\mathrm{exc}}^{(1)} = 0.455\,\mu\mathrm{A}$, excess current at high bias $I_{\mathrm{exc}}^{(2)} = 0.216\,\mu\mathrm{A}$, superconducting gap $\Delta = 87.5\,\mu\mathrm{eV}$, critical current $I_C = 260\,\mathrm{nA}$, re-trapping current $I_r = 175\,\mathrm{nA}$.

The four resistance traces in Fig. 5b converge to two different critical temperatures, $\sim 760\,\mathrm{mK}$ and $\sim 780\,\mathrm{mK}$, corresponding to the two different peak components in the resistance data. This supports the idea that the two leads have slightly different critical temperatures.

IV. DISCUSSION AND CONCLUSIONS

In the previous section we have demonstrated how one can find the dependence of the heat power emitted by the junction on the bath temperature by measuring critical voltage at which the leads switch to the normal state. This simple technique is applicable to any highly transparent Josephson junction and it might be useful for high-flux calibration of bolometers containing such junctions.

Let us now discuss the specific case of an SGS Josephson junction in more detail. We find that the critical Joule heating P_C becomes independent of the bath temperature at $T_{\mathrm{bath}} \ll T_C$, see Fig. 5b. Such saturation of the heat flow at low temperature is rather common in systems with weak coupling between electrons and lattice phonons. We find similar behavior in the theoretical electronic heat transport model of Sec. II A. Indeed, for $T_0 = T_C$ and at $T_{\mathrm{bath}} \ll T_C$, where the energy gap of the superconductor does not depend on temperature, the heat power (13) saturates.

According to Figs. 4 and 5, the saturated low-temperature critical power amounts to $P_C^{\mathrm{NS}} = 1.2\,\mathrm{nW}$ and $P_C^{\mathrm{S}} = 4.0\,\mathrm{nW}$ in our non-suspended and suspended sample, respectively. If we scale these values by the number of leads (see Table I) and the cross sectional area of the sandwich conductors, $d \times W_{\mathrm{leads}}$, we obtain the values $P_C^{\mathrm{NS}}/(d \times W_{\mathrm{leads}}) = 10.4\,\mathrm{kW/m^2}$ and $P_C^{\mathrm{S}}/(d \times W_{\mathrm{leads}}) = 13.7\,\mathrm{kW/m^2}$. The similarity of these two critical power densities supports the conclusion that thermal transport along the leads is the main mechanism of heat relaxation in our devices.

The critical voltages amount to $V_C^{\mathrm{NS}} = 0.38\,\mathrm{mV}$ and $V_C^{\mathrm{S}} = 3.0\,\mathrm{mV}$ for samples NS and S, respectively. We have applied Eq. (15) at low T to investigate whether these values scale according to the model. Since we do not know exactly the lead resistance, we compare the measured ratio of critical voltages to the theory by assuming that the lead resistance scales inversely proportional to the cross sectional area of the leads [40]. With the parameters from Table I, Eq. (15) yields for the critical voltage ratio $V_C^{\mathrm{NS}}/V_C^{\mathrm{S}} = 8.5$, while from the experimental data in Figs. 4 and 5 we obtain $V_C^{\mathrm{NS}}/V_C^{\mathrm{S}} = 7.9$. Thus, our theoretical model accounts for the variation of the critical voltage within one order of magnitude.

The observed exponent in the temperature dependence of the power for the suspended junction, $\gamma = 3.1$, is close to the one found by Borzenets *et al* for SGS junctions with Pb leads and graphene deposited on Si/SiO_2 substrate [41]. Lead has large superconducting gap, which should effectively cut off electronic thermal conductance below 1 K and leave only electron-phonon coupling for en-

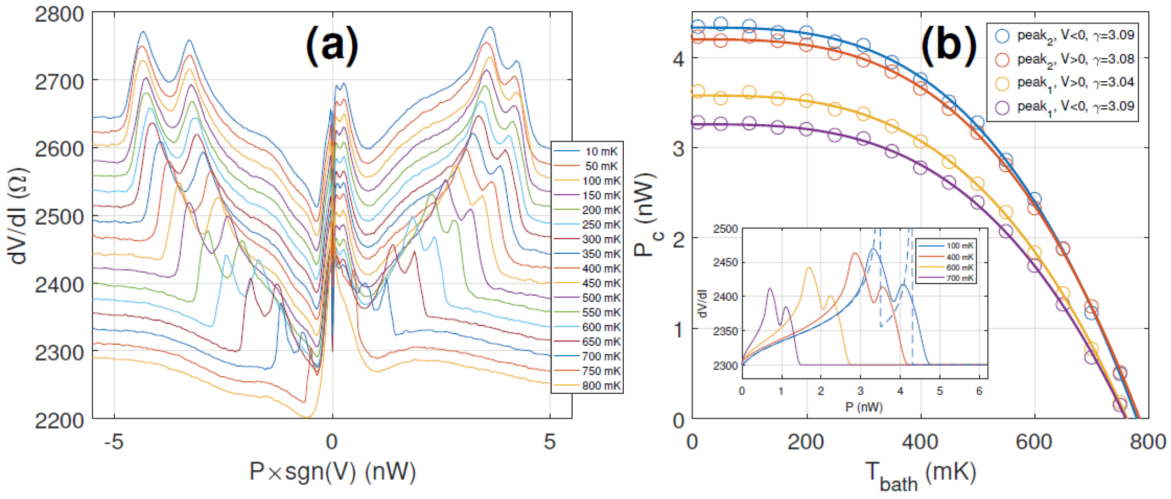

FIG. 5. Heating effects in a suspended bilayer SGS sample with the following parameters: normal state resistance $R = 2.2\,\mathrm{k\Omega}$, maximum excess current $I_{\mathrm{exc}} = 26.5\,\mathrm{nA}$, superconducting gap $\Delta \approx 80\,\mu\mathrm{eV}$, $\alpha = 0.73$. (a) Differential resistance as a function of power at different bath temperatures (successive curves have been shifted vertically by $20\,\Omega$. (b) Critical powers P_C, i.e. positions of the resistance peaks in frame 5(a), as a function of bath temperature. Continuous lines are fits using the heat flow power law in Eq. (17) with the exponent γ as a fitting parameter. All these data were measured at $V_g = -20\,\mathrm{V}$ which corresponds to a hole carrier density of $n = 2\times10^{11}\,\mathrm{cm}^{-2}$ Inset: Simulated results for the superconducting-to-normal transition due to Joule heating, where the resistance peaks arise from a reduction of excess current. Solid lines have been smoothed by a moving average, whereas the dashed blue line displays the unsmoothed result for $T_{\mathrm{bath}} = 100\,\mathrm{mK}$.

ergy relaxation [42]. Power law thermal transport with the exponent $\gamma = 4.5$ has also been observed in superconducting Nb at low temperatures $k_BT \ll \Delta$ [43].

The origing of the exponent $\gamma \approx 3$ observed in our suspended device is not fully clear. Let us briefly discuss several possible explanations for this observation. In our experiment the ratio k_BT/Δ extends to large values, and, therefore, energy relaxation should be dominated by quasiparticles carrying heat through the leads. For temperatures close to T_C the quasiparticles behave almost as normal state electrons obeying Wiedemann-Franz law, which leads to $\gamma = 2$. The increase of the exponent γ from 2 to 3 may be qualitatively explained by several different effects or by their combination. First, the quasiparticle heat current (13) is lower and more sensitive to temperature than the normal state one in the whole interval $T < T_C$, including the temperatures close to T_C. Second, the parameter R_{leads}, appearing in the cooling power (13), is the resistance of the part of an Al lead in which thermalization between the quasiparticles and the substrate phonons occurs. Since the corresponding thermalization length L_T is reduced with increasing temperature, the resistance $R_{\mathrm{leads}} \propto L_T$ is also reduced. Hence, the dependence of the power (13) on temperature becomes stronger than it were in the model with fixed R_{leads}. Yet another possibility for the increase of the exponent is the injection of strongly non-equilibrium quasiparticles with non-thermal distribution in the Al leads at high bias voltages. The propagation of such quasiparticles should be described by the full set of kinetic equations with the inclusion of charge imbalance instead of just one Eq. (10). Quantitative analysis of the effects mentioned above goes beyond the scope of this paper. At the moment, the similarity of the exponents observed in our experiment and in Ref. [41] remains puzzling.

In conclusion, we have analyzed, both theoretically and experimentally, the effect of Joule heating on the IV characteristics of highly transparent Josephson junctions. We have shown that the Joule heating supresses the excess current and induces dips in the differential conductance at bias voltages where the two leads switch to the normal state. We have derived simple analytical expressions for the shape of these dips and for their positions in a specific case of a suspended junction, which is cooled only through the leads. We have experimentally tested predictions of the theory by studing SGS junctions in both suspended and non-suspended configurations. Good agreement between the experiment and the theory is found at $T \ll T_C$. At higher temperatures we observe power law temperature dependence of the heat current instead of theoretically expected exponential dependence. Our work also indicates that excess current can be employed for thermometry in special cases.

ACKNOWLEDGEMENTS

Discussions with Manohar Kumar and Alexander Savin are gratefully acknowledged. This work was supported by the Academy of Finland projects 314448 (BOLOSE), 310086 (LTnoise) and 312295 (CoE, Quantum Technology Finland) as well as by ERC (grant no.

670743). This research project utilized the Aalto University OtaNano/LTL infrastructure which is part of European Microkelvin Platform (funded by European Union's Horizon 2020 Research and Innovation Programme Grant No. 824109). A.L. is grateful to Väisälä foundation of the Finnish Academy of Science and Letters for scholarship. The work at HSE University (M.R.S. and A.S.V.) was supported by the framework of the Academic Fund Program at HSE University in 2021 (grant No 21-04-041).

[1] W. Haberkorn, H. Knauer, and J. Richter, Phys. Status Solidi A**47**, K161 (1978).
[2] A. A. Golubov, M. Yu. Kupriyanov, and E. Il'ichev, Rev. Mod. Phys. **76**, 411 (2004).
[3] M. Hays, G. de Lange, K. Serniak, D.J. van Woerkom, D. Bouman, P. Krogstrup, J. Nygard, A. Geresdi, and M.H. Devoret, Phys. Rev. Lett. **121**, 047001 (2018).
[4] A. Zazunov, V. S. Shumeiko, E. N. Bratus, J. Lantz, and G.Wendin, Phys. Rev. Lett. **90**, 087003 (2003).
[5] M. Octavio, M. Tinkham, G.E. Blonder, and T.M.Klapwijk, Phys. Rev. B **27**, 6739 (1983).
[6] J. C. Cuevas, A. Martin-Rodero, and A. Levy Yeyati, Phys. Rev. B **54**, 7366 (1996).
[7] A. Bardas and D.V. Averin, Phys. Rev. B **56**, R8518 (1997).
[8] D.V. Averin, G. Wang, and A.S. Vasenko, Phys. Rev. B **102**, 144516 (2020).
[9] W. Liang, M. Bockrath, D. Bozovic, J. H. Hafner, M. Tinkham, and H. Park, Nature **411**, 665 (2001).
[10] P. Jarillo-Herrero, J.A. van Dam, and L.P. Kouwenhoven, Nature **439**, 953 (2006).
[11] J-D. Pillet, C. H. L. Quay, P. Morfin, C. Bena, A. Levy Yeyati and P. Joyez, Nat. Phys. **6**, 965 (2010).
[12] V.E. Calado, S. Goswami, G. Nanda, M. Diez, A.R. Akhmerov, K. Watanabe, T. Taniguchi, T.M. Klapwijk, and L.M.K. Vandersypen, Nat. Nanotechnology **10**, 761 (2015).
[13] G.-H. Lee, S. Kim, S.-H. Jhi, H.-J. Lee, Nature Comm. **6**, 6181 (2015).
[14] S. Abay, D. Persson, H. Nilsson, F. Wu, H.Q. Xu, M. Fogelström, V. Shumeiko, and P. Delsing, Phys. Rev. B **89**, 214508 (2014).
[15] E.M. Spanton, M. Deng, S. Vaitiekenas, P. Krogstrup, J. Nygard, C.M. Marcus, and K.A. Moler, Nat. Phys. **13**, 1177 (2017).
[16] I. Sochnikov, L. Maier, C.A. Watson, J.R. Kirtley, C. Gould, G. Tkachov, E. M. Hankiewicz, C. Brüne, H. Buhmann, L.W. Molenkamp, and K.A. Moler, Phys. Rev. Lett. **114**, 066801 (2015).
[17] M. Veldhorst, M. Snelder, M. Hoek, T. Gang, V.K. Guduru, X.L. Wang, U. Zeitler, W.G. van der Wiel, A.A. Golubov, H. Hilgenkamp and A. Brinkman, Nat. Mat. **11**, 417 (2012).
[18] S. Charpentier, L. Galletti, G. Kunakova, R. Arpaia, Y. Song, R. Baghdadi, S.M. Wang, A. Kalaboukhov, E. Olsson, F. Tafuri, D. Golubev, J. Linder, T. Bauch, and F. Lombardi, Nat. Comm. **8**, 2019 (2017).
[19] G. E. Blonder, M. Tinkham, and T. M. Klapwijk, Phys. Rev. B **25**, 4515 (1982).
[20] H. Vora, P. Kumaravadivel, B. Nielsen and X. Du, Appl. Phys. Lett. **100**, 153507 (2012).
[21] K. C. Fong, and K. Schwab, Phys. Rev. X **2**, 031006 (2012).
[22] J. Yan, et al., Nat. Nanotechnol. **7**, 472–478 (2012).
[23] C. McKitterick, D. Prober and B. Karasik, J. Appl. Phys. **113**, 044512 (2013).
[24] D. K. Efetov, et al., Nat. Nanotechnol. **13**, 797–801 (2018).
[25] Q. Han, et al., Sci. Rep. **3**, 3533 (2013).
[26] X. Cai, et al., Nat. Nanotechnol. **9**, 814–819 (2014).
[27] A. E. El Fatimy, et al., Nat. Nanotechnol. **11**, 335–338 (2016).
[28] G.-H. Lee, D.K. Efetov, W. Jung, L. Ranzani, E.D. Walsh, T.A. Ohki, T. Taniguchi, K. Watanabe, P. Kim, D. Englund and K.C. Fong, Nature **586**, 42 (2020).
[29] R. Kokkoniemi, J.-P. Girard, D. Hazra, A. Laitinen, J. Govenius, R. E. Lake, I. Sallinen, V. Vesterinen, M. Partanen, J. Y. Tan, K. W. Chan, K. Y. Tan, P. Hakonen and M. Möttönen, Nature **586**, 47 (2020).
[30] A.V. Zaitsev, Zh. Eksp. Teor. Fiz. **86**, 1742 (1984) [Sov. Phys. JETP **59**, 1015 (1984)].
[31] M. Titov and C. W. J. Beenakker, Phys. Rev. B **74**, 041401(R) (2006).
[32] P. Joyez, D. Vion, M. Götz, M. H. Devoret, and D. Esteve, J. Supercond. **12**, 757 (1999).
[33] O. N. Dorokhov, Solid State Commun. **51**, 381 (1984).
[34] J. Tworzydlo, B. Trauzettel, M. Titov, A. Rycerz, and C.W.J. Beenakker, Phys. Rev. Lett. **96**, 246802 (2006).
[35] J. C. Cuevas, J. Hammer, J. Kopu, J. K. Viljas, and M. Eschrig, Phys. Rev. B **73**, 184505 (2006).
[36] J. Bardeen, L.N. Cooper, and J.R. Schrieffer, Phy. Rev. **108**, 1175 (1957).
[37] J. Bardeen, G. Rickayzen, and L. Tewordt, Phys. Rev. **113**, 982 (1959).
[38] N. Tombros, A. Veligura, J. Junesch, J. J. van den Berg, P. J. Zomer, M. Wojtaszek, I. J. V. Marun, H. T. Jonkman, and B. J. van Wees, J. Appl. Phys. **109**, 93702 (2011).
[39] J. P. Pekola, K. P. Hirvi, J. P. Kauppinen, and M. A. Paalanen, Phys. Rev. Lett. **73**, 2903 (1994).
[40] The normal state resistance of the Al layer is much smaller than that of the Ti layer. Hence, we also checked the scaling using the Al layer thickness, but the difference is small, and the change would not modify our conclusions. We use the total thickness because the mechanism of the electronic heat transport in the superconducting state is not fully clear.
[41] I. V. Borzenets, U. C. Coskun, H. T. Mebrahtu, Y. V. Bomze, A. I. Smirnov, and G. Finkelstein, Phys. Rev. Lett., 111, 027001 (2013).
[42] J. Voutilainen, A. Fay, P. Häkkinen, J. K. Viljas, T. T. Heikkilä, and P. J. Hakonen, Phys. Rev. B, **84**, 045419 (2011).
[43] A. Feshchenko, O-P. Saira, J. Peltonen, J. P. Pekola, Sci Rep **7**, 41728 (2017).